Appendices

Appendix A

A.1 Soil map of Morocco (FAO, 1974)

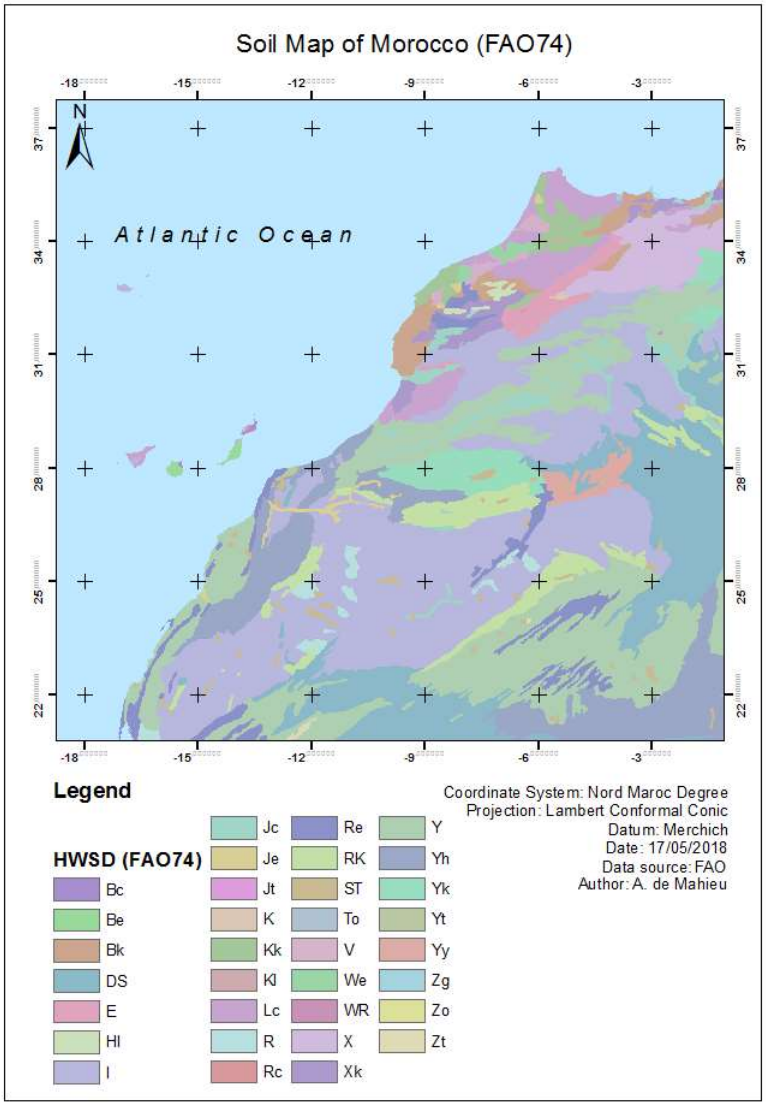

Figure A.1: Soil map of Morocco, Harmonized World Soil Database (HWSD) (FAO, 1974). Maâmora forest is characterized by chromic luvisols (Lc).

A.2 Pictures of the study area

Figure A.2: Photo n^o 1. High variability in terms of tree growth: plot 4 is located on the left side of the picture whereas plot 5 is located on the right side.

Figure A.3: Photo n^o 2.

Figure A.4: Photo n^o 3.

Figure A.5: Photo n^o 4. Trees located in plot 19.

Figure A.6: Photo n^o 5.

Figure A.7: Photo n^o 6. Trees located in plot 35. GPR measurements are recorded with the frequency domain GPR.

A.3 Preliminary maps of the study area

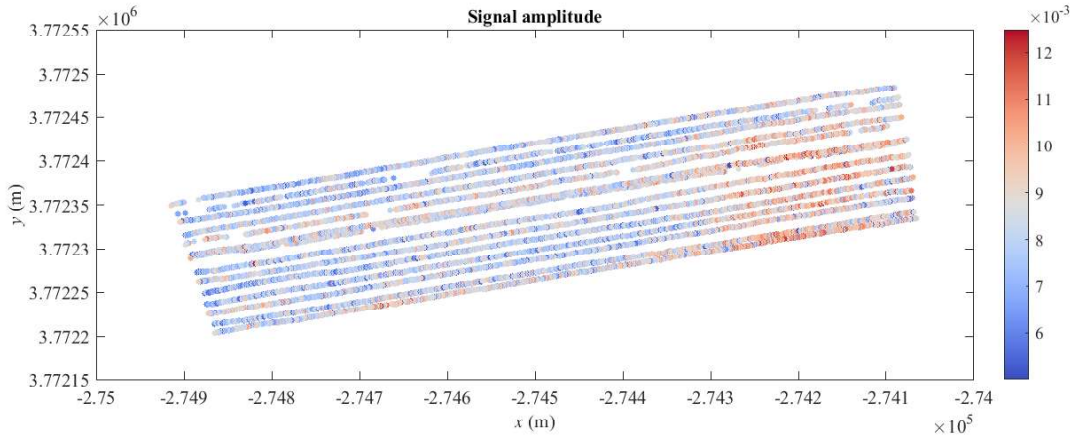

Figure A.8: Signal amplitude variation of the 14 GPR transects. Data points were recorded with the frequency domain GPR.

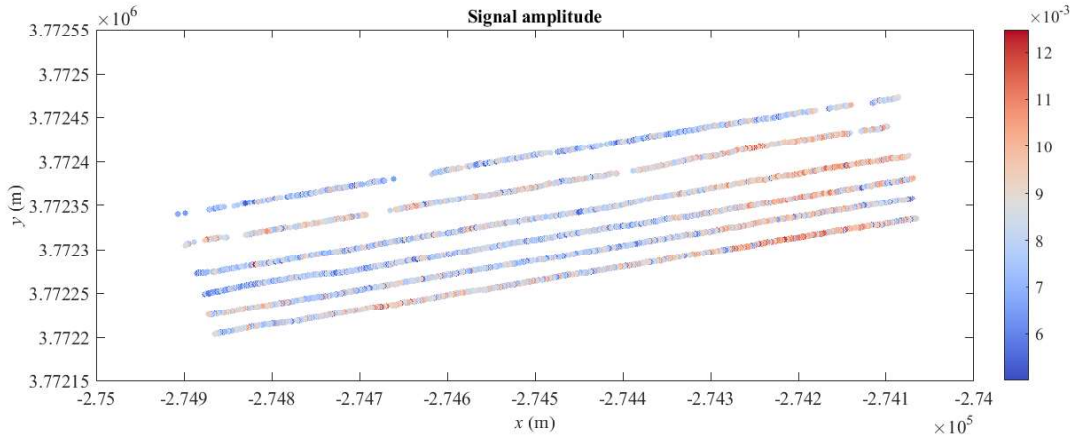

Figure A.9: Signal amplitude variation of the 6 selected GPR transects (T2, T6, T12, T18, T24 and T28). Data points were recorded with the frequency domain GPR.

A.4 Protocol of hand-touch sensation method

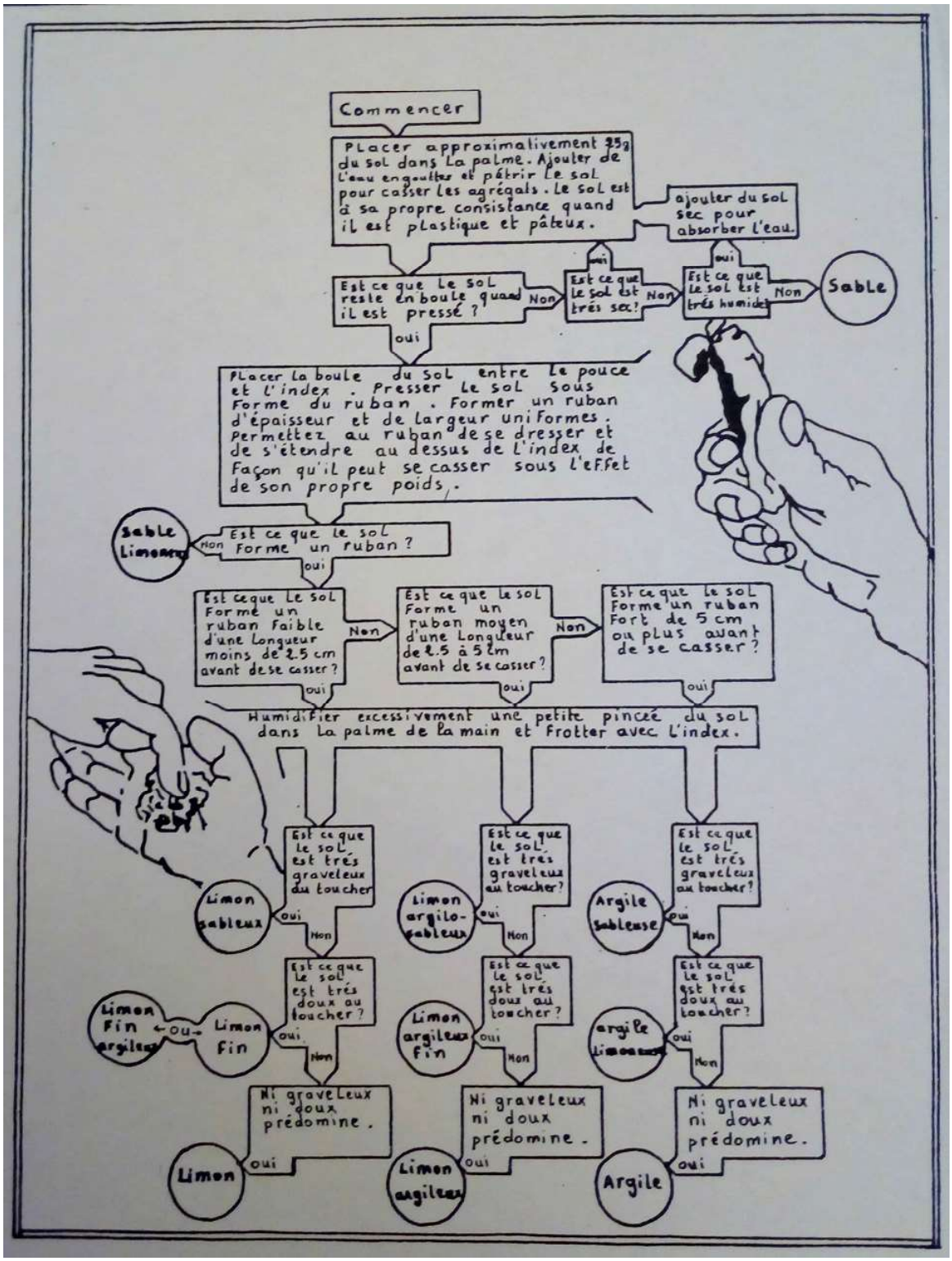

Figure A.10: Soil texture determination using the hand-touch sensation method (Hassan, B.J., Ecole Nationale Forestière d'Ingénieurs de Salé (1988)).

A.5 Total carbon content : Walkley-Black method

Mode opératoire

- Peser 2 g de sol tamisé à 0.2 mm.
- Introduire la prise de sol dans un erlenmeyer de 250 mL.
- Ajouter 15 ml de bichromate de potassium 1N.
- Agiter doucement.
- Ajouter 20 ml de H_2SO_4 concentré en agitant doucement.
- Laisser reposer une demi-heure.
- Ajouter 115 ml d'eau distillée.
- Bien homogénéiser et laisser au repos pendant 2 heures.
- Prélever ensuite 50 ml de solution surnageante dans un erlenmeyer de 250 ml.
- Ajouter 5 ml de NaF concentré.
- Ajouter 3 à 4 gouttes de diphénylamine.
- Titrer ensuite l'excès de bichromate par la solution de sel de Mohr. La couleur passe du bleu foncé au vert clair.
- Effectuer un témoin dans les mêmes conditions.

A.6 Antenna calibration of the frequency domain radar system with fiberglass handle

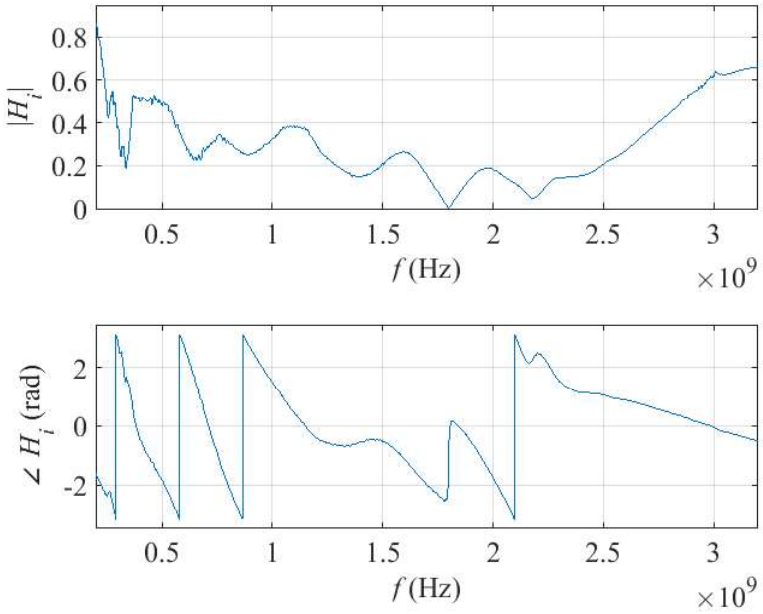

Figure A.11: Complex return loss transfer function, H_i.

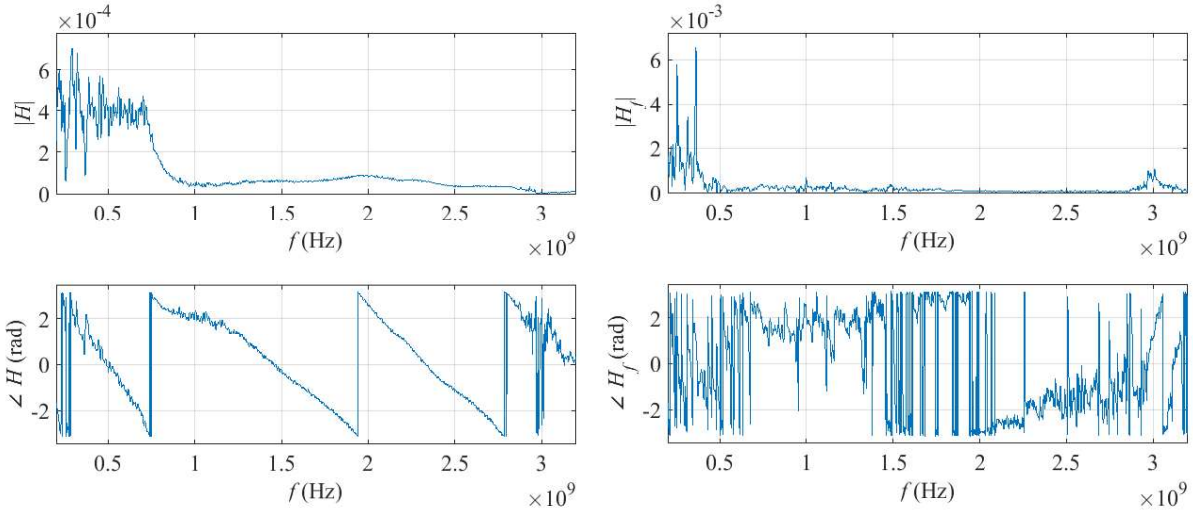

(a) (b)

Figure A.12: Transfer functions. (a) Combination of the transmitting (H_t) and receiving (H_r) transfer functions, H. (b) Feedback loss transfer function, H_f

A.7 Laboratory tests of the frequency domain radar system on top of a sandbox

A.7.1 Antenna height over the sandbox: 1.5 cm

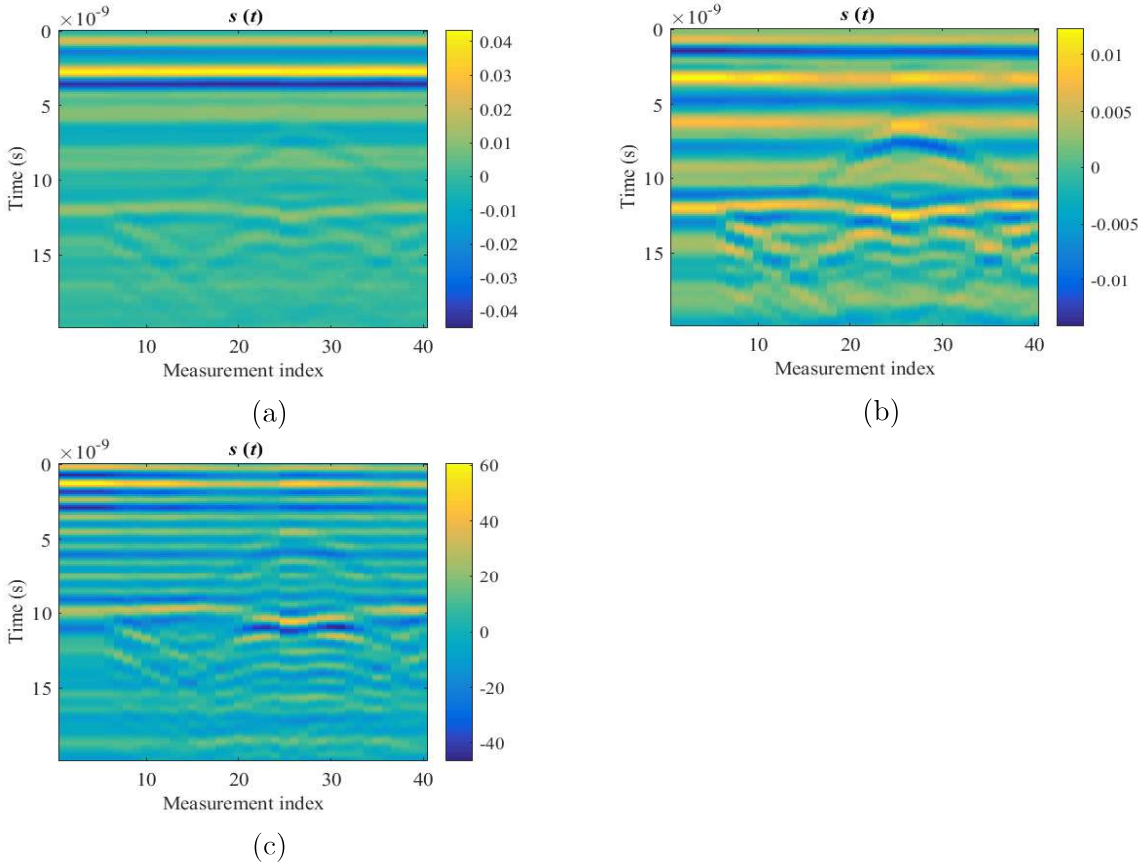

Figure A.13: Radar images over the sandbox with the antenna situated at 1.5 cm from the sand surface. (a) Raw radar data. (b) Radar data from which H_i has been subtracted. (c) Radar data from which antenna effects have been filtered out using the radar equation.

A.7.2 Antenna height over the sandbox: 10 cm

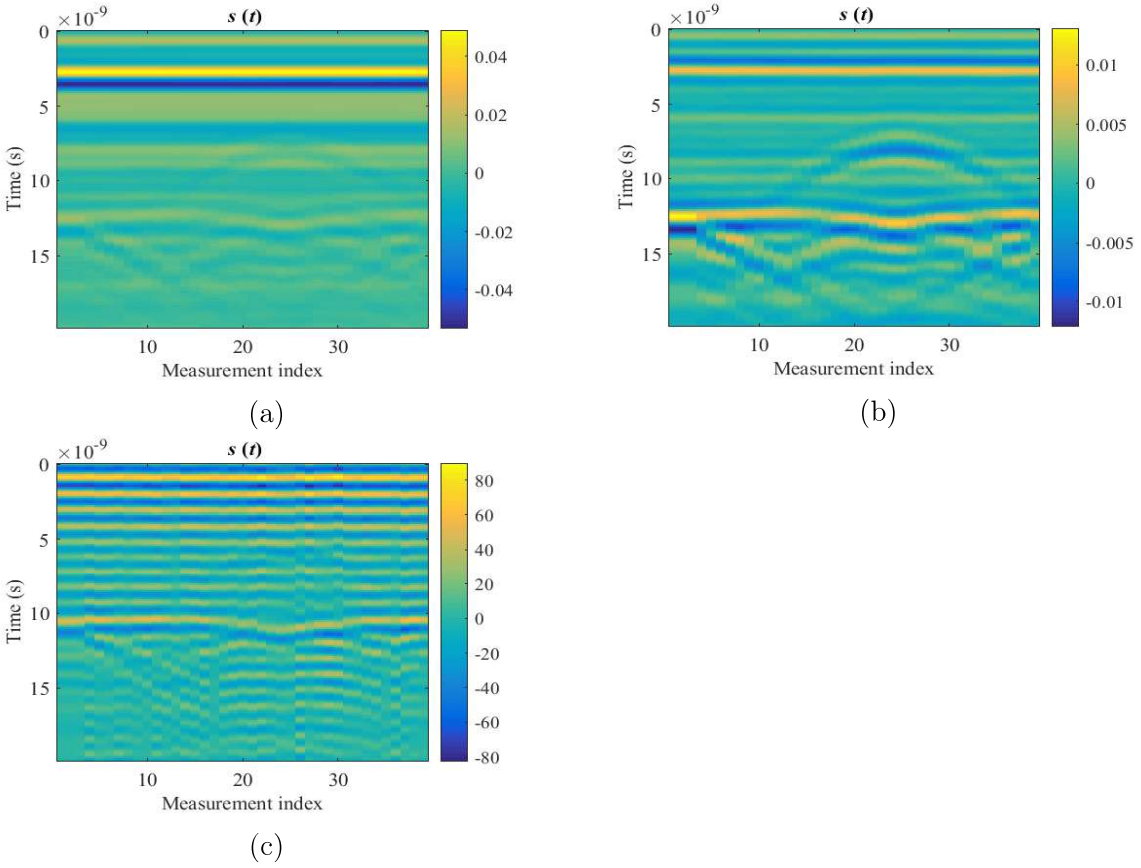

Figure A.14: Radar images over the sandbox with the antenna situated at 10 cm from the sand surface. (a) Raw radar data. (b) Radar data from which H_i has been subtracted. (c) Radar data from which antenna effects have been filtered out using the radar equation.

A.7.3 Antenna height over the sandbox: 20 cm

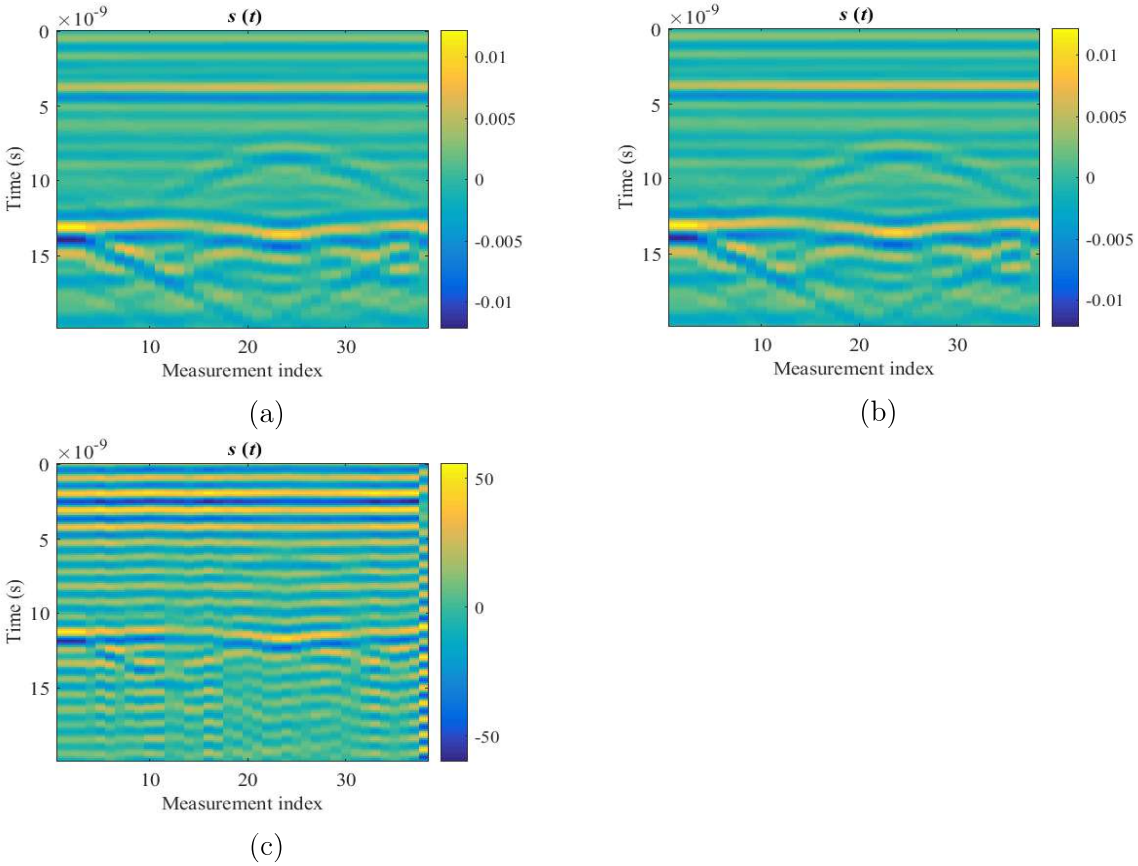

Figure A.15: Radar images over the sandbox with the antenna situated at 20 cm from the sand surface. (a) Raw radar data. (b) Radar data from which H_i has been subtracted. (c) Radar data from which antenna effects have been filtered out using the radar equation.

A.7.4 Antenna height over the sandbox: 40 cm

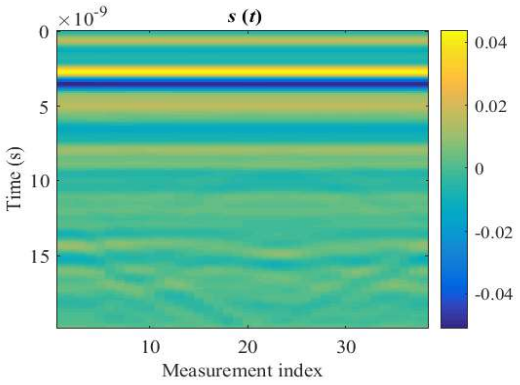

(a) Radar image without filter

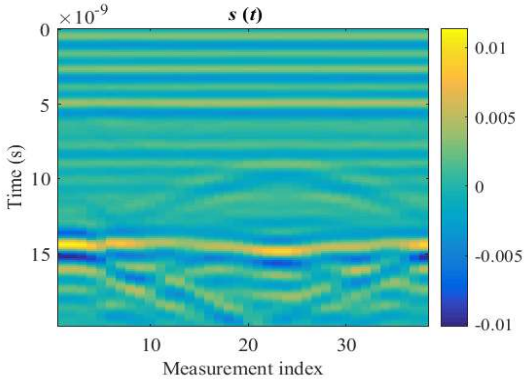

(b) Radar image with Hi filter

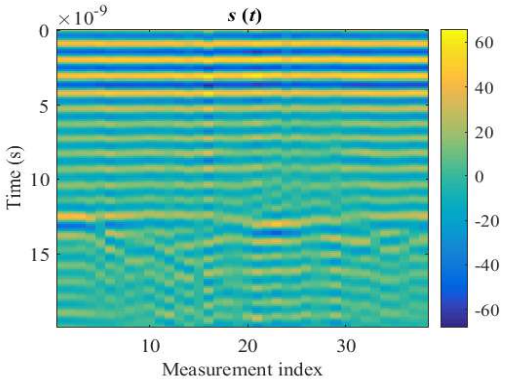

(c) Radar image with Hi, H and Hf filters

Figure A.16: Radar images over the sandbox with the antenna situated at 40 cm from the sand surface. (a) Raw radar data. (b) Radar data from which H_i has been subtracted. (c) Radar data from which antenna effects have been filtered out using the radar equation.

A.8 Relative dielectric permittivity map

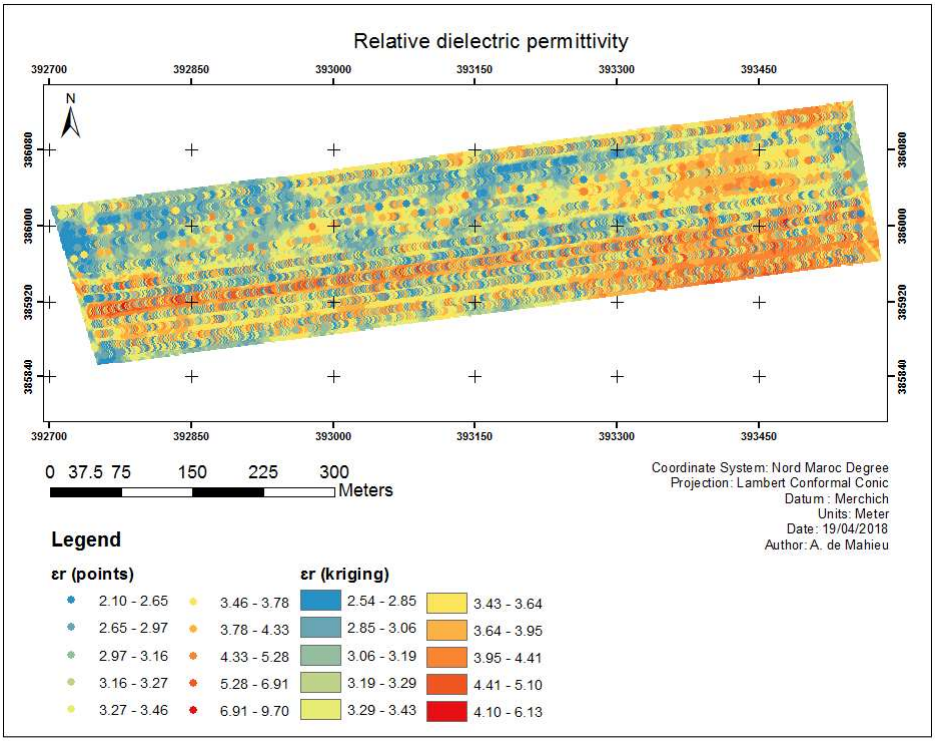

Figure A.17: Map of the relative dielectric permittivity (ε_r) data points stacked on top of the map obtained by applying the kriging method.

Input datasets

Dataset	C:\Users\Aurore Dell\Documents\ArcGIS\Mémoire Maamora.mdb\1904_epsr
Type	Feature Class
Data field 1	epsr
Records	13666

Method	**Kriging**
Type	Ordinary
Output type	Prediction
Dataset #	1
Trend type	None
Searching neighborhood	Standard
Neighbors to include	25
Include at least	5
Sector type	Four and 45 degree
Major semiaxis	9.495431211291663e-005
Minor semiaxis	9.495431211291663e-005
Angle	0
Variogram	Semivariogram
Number of lags	12
Lag size	2.0246128743076606e-005
Measurement error %	100
Model type	Exponential
Range	3.2066685583095374e-006
Anisotropy	No
Partial sill	1.041699664961

Figure A.18: Parameters of the kriging method applied on *ArcGIS*.

A.9 Radar images of 2015 using a time domain commercial GPR

The first transect comprises sub-transects 2A, 2B and 1 (direction SW - NE) and the second transect comprises sub-transects 5, 4, 3 and 2 (direction SW - NE) (see Figure 3.5).

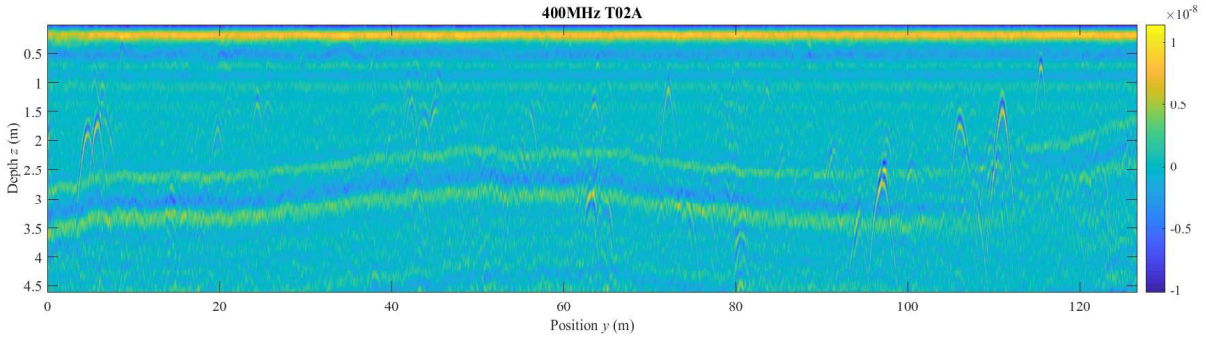

Figure A.19: Sub-transect 2A (with GSSI positioning wheel)(Dr F. André, 2015).

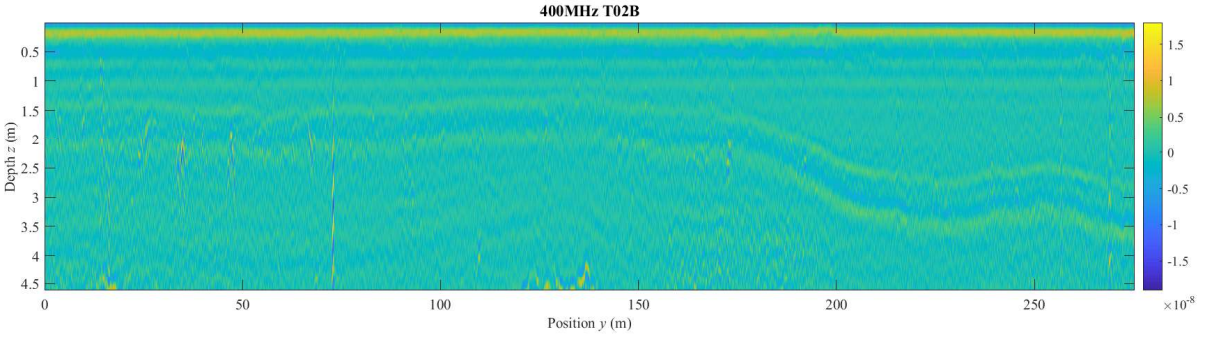

Figure A.20: Sub-transect 2B (with GSSI positioning wheel)(Dr F. André, 2015).

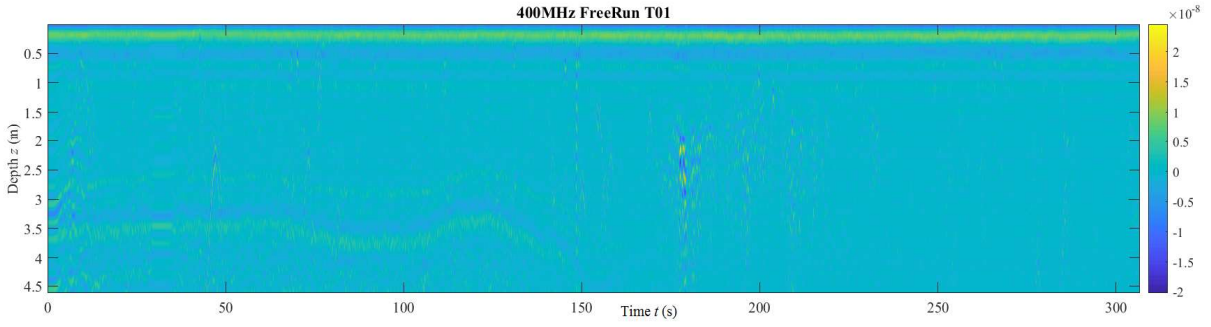

Figure A.21: Sub-transect 1 (Free Run)(Dr F. André, 2015).

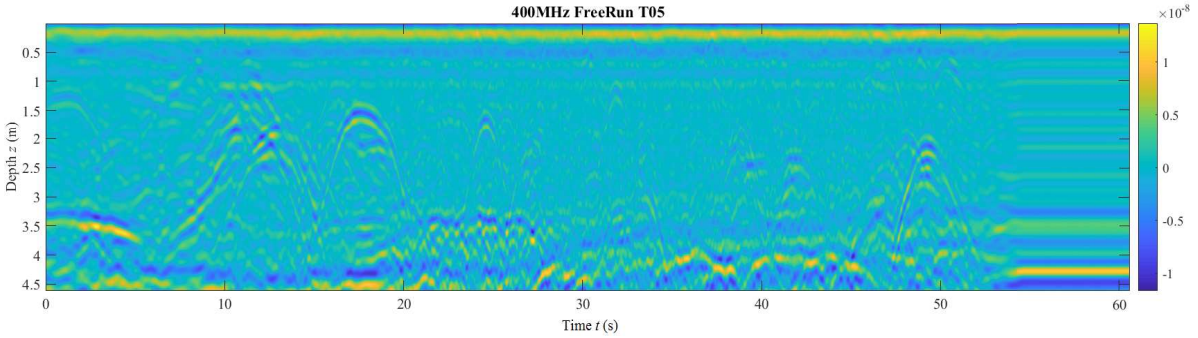

Figure A.22: Sub-transect 5 (Free Run)(Dr F. André, 2015).

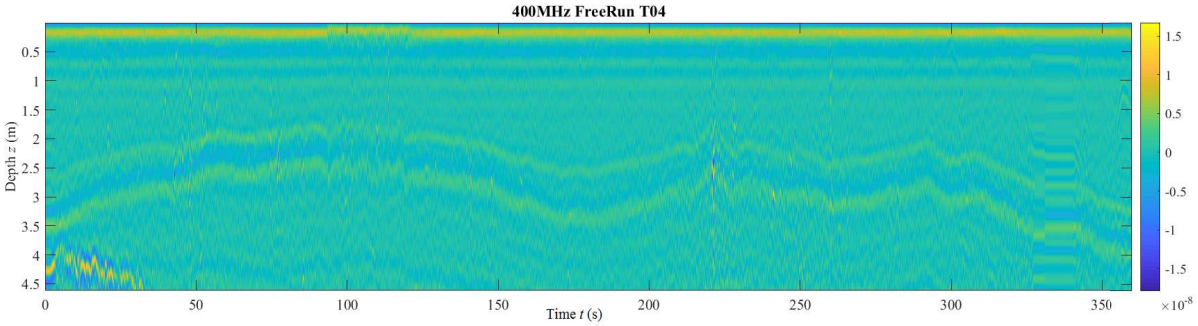

Figure A.23: Sub-transect 4 (Free Run)(Dr F. André, 2015).

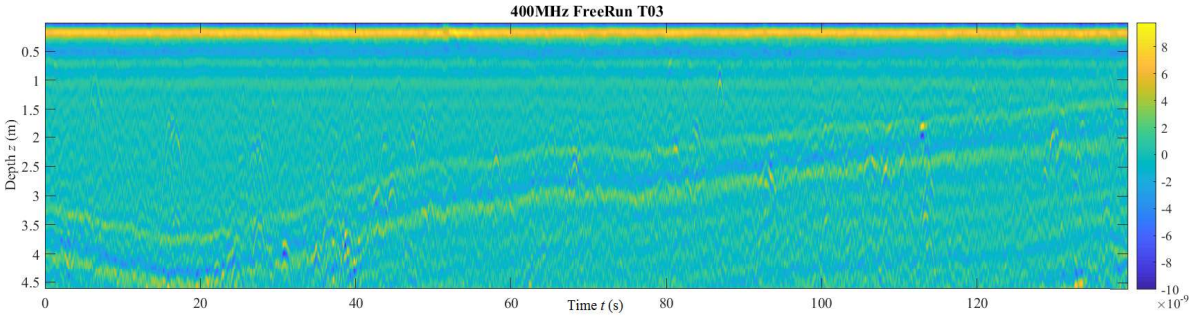

Figure A.24: Sub-transect 3 (Free Run)(Dr F. André, 2015).

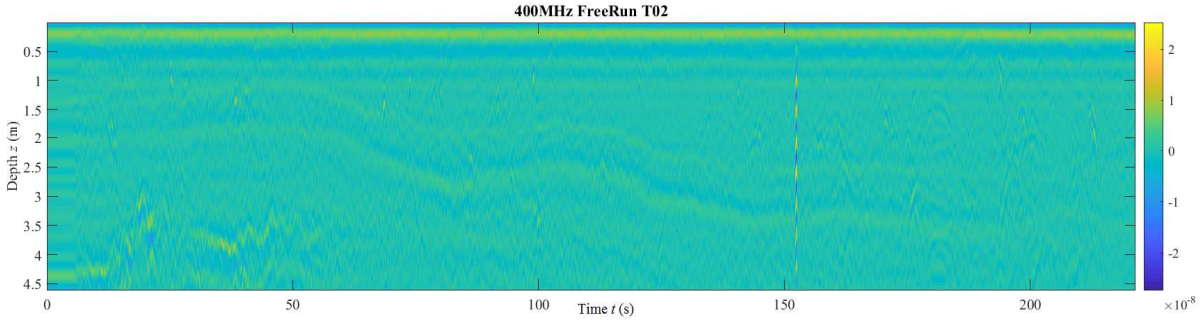

Figure A.25: Sub-transect 2 (Free Run)(Dr F. André, 2015).

A.10 Water content in soil samples

Table A.1: Laboratory analyses at the soil laboratory of the National School of Forest Engineers (ENFI), Salé (Morocco). Gravimetric soil water content (θ_v) of three soil samples per profile.

Plot	Depth [cm]	θ_v[%]	Plot	Depth [cm]	θ_v[%]	Plot	Depth [cm]	θ_v[%]
	0-20	6.76		0-40	6.26		0-40	7.72
1	160-180	6.16	13*	80-100	5.64	25	160-180	6.95
	200-220	9.79		200-220	12.34		200-220	14.26
	0-20	6.39		0-40	7.06		0-40	7.00
2	160-180	10.00	14**	100-120	5.34	26	160-180	11.30
	200-220	6.57		180-200	16.01		200	12.82
	0-20	5.57		0-20	6.81		0-20	6.41
3	140-160	3.00	15**	160-180	6.89	27	120-160	5.99
	180-200	3.35		200-220	15.35		220	13.70
	0-20	5.78		0-40	5.94		0-40	6.54
4	140-160	2.36	16**	140-160	5.92	28*	120-140	7.20
	200-220	2.64		200-220	15.78		180-200	17.22
	0-20	5.52		0-60	5.68		0-40	5.70
5	140-160	4.85	17**	120-140	6.29	29*	140-160	13.30
	200-220	10.50		200	17.76		160-180	15.25
	0-20	5.38		0-40	6.95		0-40	6.39
6	140-160	6.22	18**	140-160	12.68	30*	120-140	18.39
	200-220	12.50		180-220	21.11		160-180	18.57
	0-20	5.72		0-40	4.80		0-20	6.36
7	140-160	14.44	19	100-120	4.80	31*	100-120	7.99
	200-220	20.85		200-220	7.47		140-160	14.50
	0-40	5.62		0-40	5.35		0-40	6.87
8	140-160	8.75	20	100-120	5.09	32*	80-100	6.19
	180-200	15.06		200-220	8.04		120-140	17.02
	0-20	5.44		0-40	5.06		0-20	8.15
9	60-100	5.12	21	140-160	5.29	33*	100-120	6.41
	200-220	15.37		180-220	15.89		160-180	13.87
	0-40	4.81		0-40	5.11		0-20	6.51
10	160-180	8.33	22	120-140	6.00	34*	120-140	6.83
	200-220	16.37		220	14.34		180-220	11.45
	0-40	5.97		0-40	5.43		0-40	6.79
11	120-140	7.62	23	140-160	6.14	35*	140-160	7.14
	180-200	17.09		180-220	13.39		180-200	13.05
	0-20	5.76		0-40	4.94		0-20	9.29
12	100-120	7.27	24	100-120	4.84	36*	140-160	8.11
	180-200	16.52		200-220	14.73		200-220	11.39

* Rainfall the previous night (25/01/2018)

** Rainfall the two previous nights (25/01/2018 and 26/01/2018)